A Brain MR Image Segmentation Method Based on DA-Unet and Superpixel

Mengxin Li[1],Xujing Zhang[2],Kexue Hu[3],Kefu Li[4],Chaoyu Han[5] ,Xinghua Wang[6]

Shenyang Jianzhu University, Shenyang110168, China

[2]Corresponding author：Xujing Zhang

E-mail: [1]*limengxin@sjzu.edu.cn*, [2]*1198808489@qq.com*, [3]*1513823267@qq.com*, [4]*1317201638@qq.com*, [5]*2692896880@qq.com*, [6]*1836907365@qq.com*

Abstract

The study of brain MR images plays an important role in assistant diagnosis and therapy. This paper proposed a method combining Unet and superpixel to segment brain MR images. First, refer to DenseNet to improve the Unet structure, and design Dense-Unet to segment the brain image. Then, based on the characteristics of brain MR images, the probability density of the membership degrees of different tissues of the pixels in the image is estimated，and the membership degree is used as a new feature to propose a linear spectrum clustering superpixel segmentation algorithm based on probability density.The segmentation result of Dense-Unet is reflected to classify the super pixel block to achieve the segmentation effect. Make full use of the high accuracy of the convolutional neural network, and the characteristics of superpixel segmentation with clear contours and edge fit. The results show that compared with the traditional brain MR segmentation algorithm, this method has a certain degree of anti-noise, and has improved effect and accuracy of edge detail.

Key words： Brain tissue segmentation； Deep Learning； DenseNet； Linear spectral clustering superpixel

1. Introduction

As the center of the nervous system, the brain controls all life activities of the human body. If the brain is abnormal, it will inevitably cause great disaster to the individual. In recent years, with the development of medical imaging technology, through equipment such as magnetic resonance imaging (Magnetic Reson-Brain imaging, MR) and Computed Tomography (CT) provide convenience for diagnosis and treatment [1].Brain MR images can be roughly divided into three parts: brain white matter, brain gray matter and cerebrospinal fluid [2]. Using image segmentation technology can realize fast and accurate automatic segmentation and assist doctors in examination, saving time and effort.

In recent years, many scholars use various methods from multiple directions. The threshold segmentation method [3] uses the preset gray amplitude as the threshold for segmentation. Based on the edge detection method [4], including active contour model and edge detection algorithm, the target is segmented by using the information of region and boundary. Region based segmentation methods [5,] such as region growth algorithm, watershed algorithm, etc. Segmentation methods based on clustering algorithm, such as K-mean clustering, Fuzzy C-means (FCM) clustering [6]. The membership degree of each pixel is calculated, the objective function is minimized, and the fuzzy classification of each organization is realized through
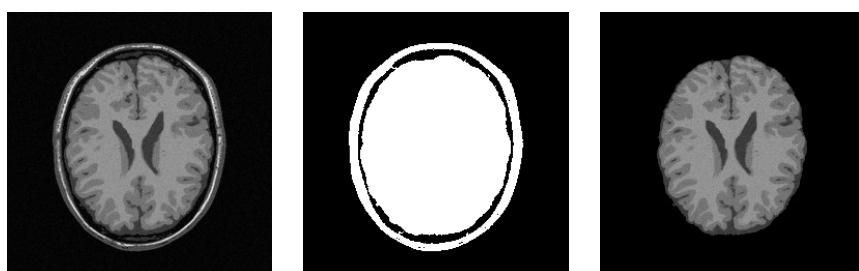
multiple iterations. This method is suitable for the situation of fuzzy and uncertain boundary in brain MR images, and has always been a popular method to study brain MR image segmentation. However, the disadvantage of FCM is also obvious. It is an unsupervised learning method, which can not use the information between pixels and is very sensitive to noise. Therefore, it is common to optimize and improve the objective function [7] or membership function [8] of FCM in combination with spatial information in recent years.

With the rise of artificial intelligence, the application of deep learning method in the field of medical images [9-11] has achieved good results. In this paper, a brain MR image segmentation method combining depth learning and Superpixel segmentation is proposed. Based on the framework of Unet network, this method improves the design of Unet with reference to deep learning models such as DenseNet and ASPP module, and obtains DA-Unet. At the same time, the image is Superpixel segmented. Based on the on-line spectral clustering Superpixel segmentation algorithm, by analyzing the characteristics of brain MR image, the probability density of pixel gray value to different tissue structures is introduced, and a linear spectral clustering Superpixel segmentation method based on probability density weighting is designed. Using the high segmentation accuracy of DA-Unet and the high fitting accuracy of Superpixel segmentation in edge contour, the result of pixel block classification is achieved by mapping the brain tissue segmentation result of DA-Unet to the Superpixel segmentation map.

2. Brain MR image segmentation
2.1 Pre-treatment

In addition to the structures of various parts of brain tissue, the normal brain MR image also includes the peripheral skull and scalp. The existence of these non brain tissue components may affect the subsequent processing, so it is necessary to preprocess and eliminate the skull part. Here, the regional growth method is used [12]. Firstly, set the appropriate threshold, select the seed pixels as the growth points, and then aggregate the qualified pixels around the seed points to make these pixels with similar characteristics form the region. Continue this process until all qualified pixels are screened out, so as to completely extract the skull region. After further processing, the brain MR image with only intracranial tissue was obtained. The results are shown in Figure 1.

(a) Original brain MR image   (b) skull region extraction   (c) skull separation

Fig.1 image preprocessing of brain MR image

2.2 Brain MR image segmentation based on DA-Unet
2.2.1 Basic Unet model

Unet network was improved and designed by Ronneberger et al. [13] on the basis of full convolution

network (FCN). It adopts the traditional Encoder-Decoder structure. The encoder extracts features through convolution pooling and other operations. The decoder restores the image through up sampling, including jump connection for feature fusion. This structure improves the loss of up sampling information and edge blur in FCN. Because Unet only needs small-scale data samples to train and obtain high-precision segmented images, it is often used in the field of medical image segmentation.

2.2.2 Dense network DenseNet

In 2017, Huang et al. [14] designed DenseNet based on the idea of residual network. It adopts short-circuit connection mechanism to strengthen the information transmission between all layers by connecting all layers, so as to ensure the lossless transmission of information in the network to the greatest extent, and reduce the network parameters to a certain extent.

DenseNet is mainly composed of Dense Block and Transition Layer. The former is an important unit of the network. Each Dense Block contains several convolution layers. The input of each convolution layer is the splicing of the output of all previous layers. The composition order of convolution layer is batch Standardization (BN), activation function (ReLu) and convolution (Conv). For a Dense Block of an L-layer, the number of all connections between layers $\frac{L(L+1)}{2}$ is. Fig. 2 is a schematic diagram of a five layer Dense Block connection structure.
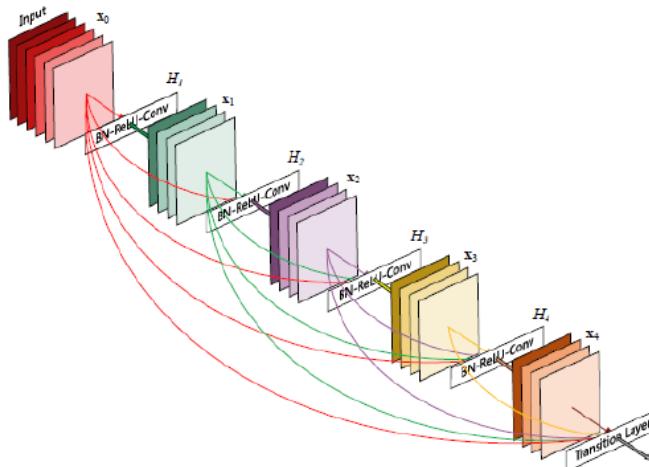

Fig.2 Structure diagram of Dense Block

Thus, DenseNet is composed of several Dense Blocks, and its formal output expression is shown in formula (1):

$$x_l = H_l\left(\left[x_0, x_1, \cdots, x_{l-1}\right]\right) \qquad (1)$$

Where x_0 to x_{L-1} represent the number of input layers of the network, H_l is the BN-ReLu-Conv transform acting on layer l, $[x_1, x_2,..., x_{L-1}]$ represents that the output characteristic diagrams from layer 0 to layer $l-1$ are spliced according to channels to obtain the total characteristic diagram.

2.2.3 ASPP module for multi-scale feature extraction

Receptive field represents the perception range of neurons in the network to the original image. The

conventional convolution kernel is small and compact, so the receptive field is relatively small, and the introduction of cavity convolution can increase the receptive field and obtain more details without increasing the number of parameters.

The structure of the Atrous Spatial Pyramid Pooling (ASPP) module in DeepLab v3 [15] is shown in Figure 3. The ASPP module uses parallel cavity convolution with different cavity ratios to extract the feature map, and obtains multi-scale feature images through feature fusion, so as to improve the network performance.
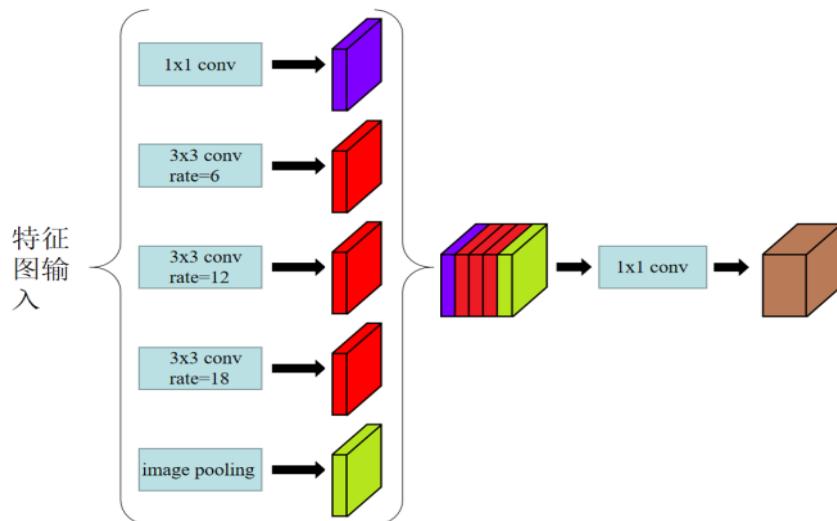

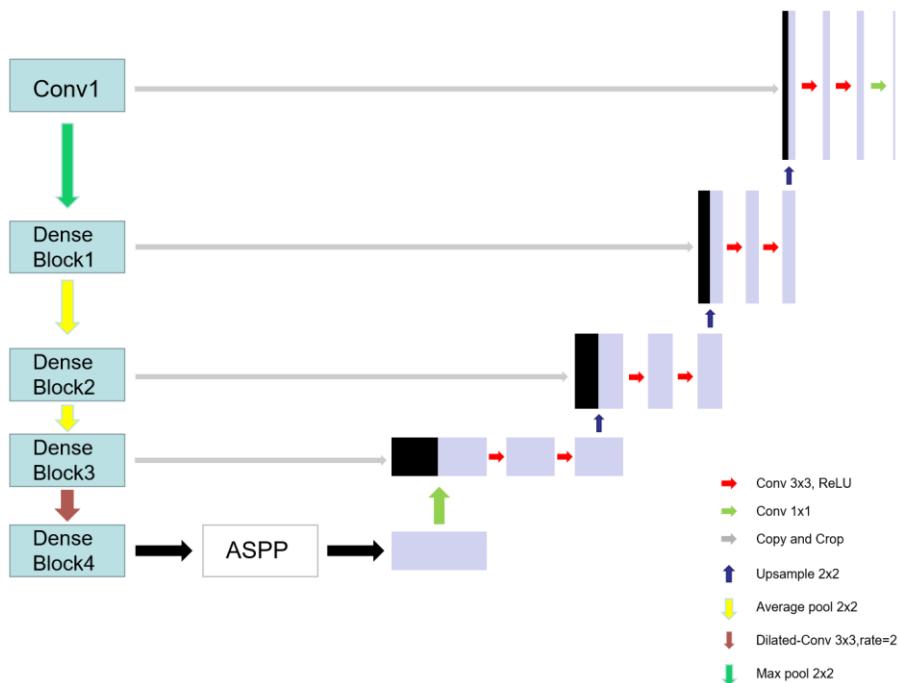**Fig. 3** structure diagram of ASPP

Fig.4 DA-Unet structure diagram

2.2.4 DA-Unet model

In the ideal state, with the increase of the number of layers, the expression ability of the deep convolution network is enhanced. The more data obtained, the better the segmentation effect. However, because the network is generally trained by gradient descent algorithm, too deep network may lead to gradient disappearance and network degradation, and the output accuracy will decline. In order to increase the network depth and improve the segmentation accuracy, and considering the poor segmentation effect of Unet on small-size targets, this paper improves Unet with reference to DenseNet structure and ASPP module, and proposes DA-Unet. The network structure and specific structural parameters are shown in Figure 4 and Table 1.

Table 1 structural parameters of DA-Unet

Layer name	Output size	Encoder(k=32)
Convolution	256×256	Conv 3 × 3
Pooling	128×128	Max pool 2 × 2,stride 2
Dense Block1	128×128	$\left[\begin{array}{l}\text{Conv } 1 \times 1, 4k \\ \text{Conv } 3 \times 3, k\end{array}\right] \times 6$
Transition Layer1	128×128	Conv 1 × 1
	64×64	Average pool 2 × 2,stride 2
Dense Block2	64×64	$\left[\begin{array}{l}\text{Conv } 1 \times 1, 4k \\ \text{Conv } 3 \times 3, k\end{array}\right] \times 12$
Transition Layer2	64×64	Conv 1 × one
	32×32	Average pool 2 × 2,stride 2
Dense Block3	32×32	$\left[\begin{array}{l}\text{Conv } 1 \times 1, 4k \\ \text{Conv } 3 \times 3, k\end{array}\right] \times 32$
Transition Layer3	32×32	Conv 1 × 1
Dilated Convolution	32×32	Dilated-Conv 3 × 3,rate=2
Dense Block4	32×32	$\left[\begin{array}{l}\text{Conv } 1 \times 1, 4k \\ \text{Conv } 3 \times 3, k\end{array}\right] \times 32$
Center	32×32	ASPP(rate=1,4,8,12,image pooling)
Convolution	32×32	Conv 1 × one
	32×32	Sum with Dense Block3
Convolution	32×32	Conv 3 × 3
Upsampling Layer1	64×64	Upsample 2 × 2
	64×64	Sum with Dense Block2
Convolution	64×64	Conv 3 × 3
Upsampling Layer2	64×64	Upsample 2 × 2
	128×128	Sum with Dense Block1
Convolution	128×128	Conv 3 × 3
Upsampling Layer3	256×256	Upsample 2 × 2
	256×256	Sum with Conv1
Convolution	256×256	Conv 3 × 3
Convolution	256×256	Conv 1 × 1

In the encoder part of DA-Unet, we mainly refer to the network structure of DenseNet-169. It should be noted that DenseNet starts with the traditional Initial Block with a step of 7 of 2×7 convolution followed by a 3 with a step size of 2×3. Maximize pooling. However, continuous down sampling will lose feature information, and it is difficult to recover the details in the subsequent decoding stage, so the initial reference Unet and Transition Layer adopts a step of 3 with a step of 1×3 convolution and step 2×2 average pool start network. In order to reduce the loss of image information caused by excessive pooling as much as possible, with reference to the design in DeepLab v3, between Dense Block3 and Dense Block4, that is, the Transition Layer3 on the upper layer of ASPP module, the lower sampling pooling cancels the use of hole convolution with hole rate of 2. Other modules, such as the number of layers of Dense Block and the learning rate k = 32, follow the structural design of DenseNet-169 without adjustment.

After that, the ASPP module is added in the middle of the encoder and decoder, but after the brain MR image is pooled three times by the encoder, the image size becomes 1 / 8, that is, 32×32 pixels. The original hole ratios 6, 12 and 18 of ASPP module are too large. Here, make some minor adjustments and reset them to 4, 8 and 12. one $\times$ The convolution and global average pooling layer of 1 are not changed. The decoder part refers to Unet, and the feature images of the same size are fused through jump connection. However, in order to reduce the amount of calculation and the number of feature images, 1 is adopted after feature fusion $\times$ 1, followed by 3×3 convolution to extract features and obtain the feature map with the same input size.

Different from the traditional image classification problem of Unet, brain MR image segmentation is a multi classification problem of brain white matter, brain gray matter, cerebrospinal fluid and background. At first, the cross entropy loss function was used in the experiment, and the effect was not ideal. After the experiment, the loss function decided to adopt Lovász Softmax Loss with more stable multi classification [16].

Lovász Softmax Loss loss is a loss function specially designed for pixel level segmentation. It is designed by using convex function lov á SZ extension to extend and continuous Jaccard loss. In multi classification image segmentation, softmax function is used to output probability distribution. At this time, the error of category $m(c)$ c is defined as:

$$m_i(c) = \begin{cases} 1 - f_i(c) & if \quad c = y_i^* \\ f_{i(c)} & otherwise \end{cases}$$

(2)

Then the loss of category C is:

$$loss(f(c)) = \overline{\Delta_{J_c}}(m(c))$$

(3)

Finally, take the average according to the category. The expression of Lovász Softmax loss is shown in equation (4):

$$loss(f(c)) = \frac{1}{|C|} \sum_{c \in C} \overline{\Delta_{J_c}}(m(c))$$

(4)

The segmentation effect of brain MR image based on DA-Unet is shown in Fig. 5. It can be seen that DA-Unet has higher accuracy and more natural edge contour than Unet. It also has better segmentation effect for small-scale targets, such as small pieces of cerebrospinal fluid and white matter in gray matter.
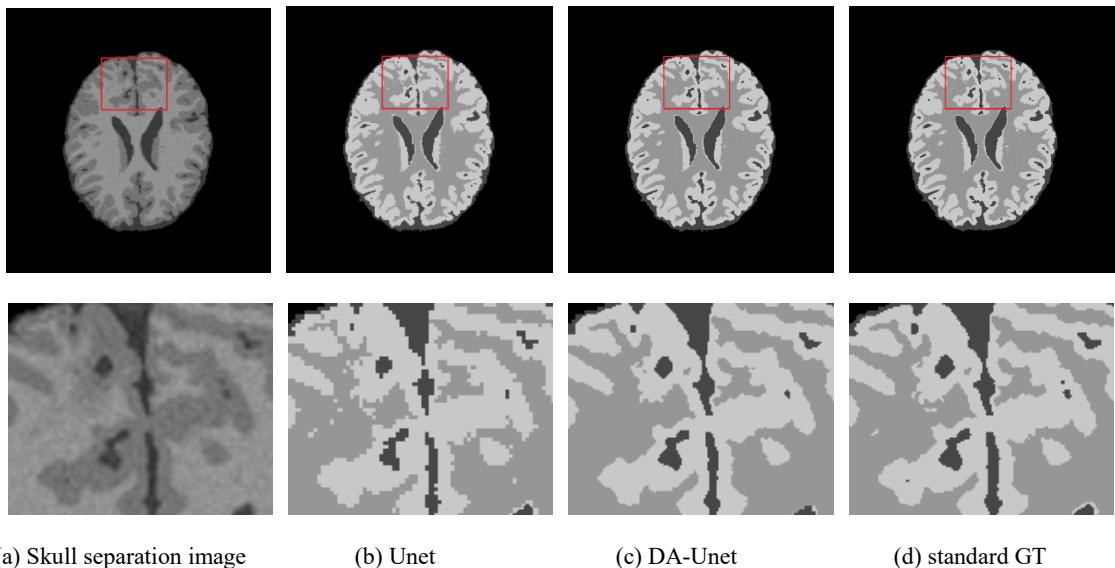
(a) Skull separation image   (b) Unet   (c) DA-Unet   (d) standard GT

Fig. 5 brain tissue segmentation results based on different methods

2.3 Brain MR image segmentation based on super pixels

2.3.1 Linear spectral clustering Superpixel segmentation

Super pixel segmentation is a segmentation method that aggregates pixels with similar color and texture features in an image to form pixel blocks. Linear spectral clustering (LSC) algorithm is a Superpixel segmentation algorithm based on linear approximation to NCuts proposed by Chen Jiansheng et al. [17] in 2017 after studying the relationship between weighted K-means and NCuts.

The cost function of weighted K-means is shown in equation (5)

$$F_{km} = \sum_{k=1}^{K} \sum_{m \in \pi_k} w(m) \left\| \phi(m) - m_k \right\|^2$$

(5)

Where:

$$m_k = \frac{\sum_{n \in \pi_k} w(n)\phi(n)}{\sum_{n \in \pi_k} w(n)}$$

m,n is the two pixel points in the image and $\omega(m)$ the weight assigned to point m. K is the number of sets, π_k which refers to the k ($k = 1,2,..., K$) set. ϕ Function can map pixel information to high-dimensional feature space. m_k is the π_k center of.

The cost function of NCuts is shown in equation (6)

$$F_{Ncuts} = \frac{1}{K} \sum_{k=1}^{K} \frac{\sum_{m \in \pi_k} \sum_{n \in \pi_k} w(m,n)}{\sum_{m \in \pi_k} \sum_{n \in V} w(m,n)}$$

(6)

When the similarity $W(m, n)$ simultaneously satisfies equation (7) (8).

$$w(m)\phi(m) \cdot w(n)\phi(n) = W(m,n), \forall m,n \in V \tag{7}$$

$$w(m) = \sum_{n \in V} W(m,n), \forall m \in V \tag{8}$$

The objective function F_{km} of weighted K-means and the objective function F_{Ncuts} of NCuts are equivalent. At this time, the equivalent function is shown in equation (9). Then, the designed kernel function is $\phi(m)$ used to map the pixel values to the ten dimensional feature space. At this time, each point is a multi-dimensional vector. Clustering these pixels can achieve the segmentation effect.

$$F_{km} = C - \sum_{k=1}^{K} \frac{\sum_m \sum_n W(m,n)}{\sum_m \sum_{n \in V} W(m,n)} = C - K \times F_{Ncuts} \tag{9}$$

In order to make the Superpixel method obtain better segmentation effect on brain MR image, combined with the characteristics of different gray peaks of brain tissue, a new Superpixel segmentation algorithm is designed based on LSC, and a probability density weighted linear spectral clustering (p-LSC) Superpixel segmentation algorithm is designed.

2.3.2 Gray level histogram statistics and probability density estimation of brain tissue

Brain tissue is mainly composed of gray matter, white matter and cerebrospinal fluid. There are certain differences in the gray values of the three parts. The gray value difference of the image is also an important basis for doctors to judge different brain tissues. Here, the histogram data obtained from the gray value statistics of 40 brain MR images is shown in Fig. 6. The x-axis is the gray value range, the y-axis is the number of pixels, and green, red and blue represent cerebrospinal fluid, gray matter and white matter respectively.
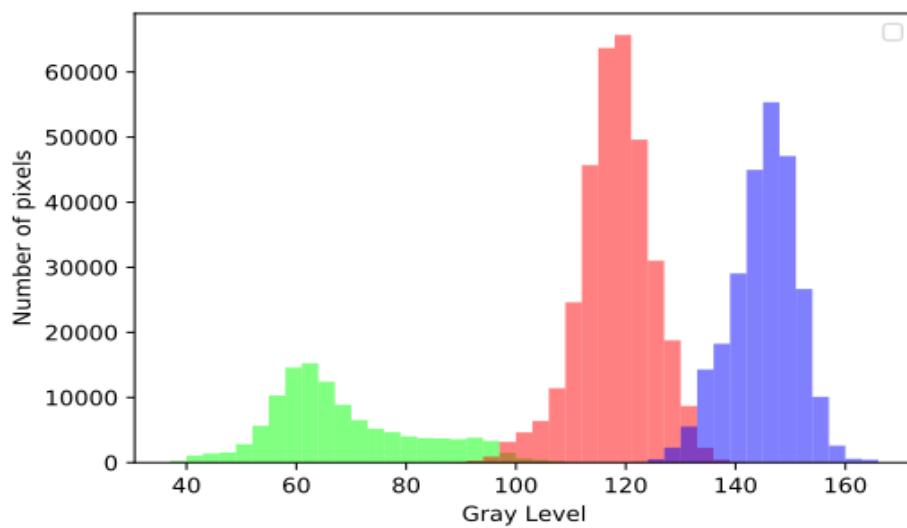

Fig. 6 Histogram statistics

It can be seen from the statistical histogram that the pixel gray values of different tissues of brain MR images are obviously different, but there are also some overlapping places . For   example, when the gray value is 90, it may be cerebral gray matter or cerebrospinal fluid. If it is distinguished solely by gray value,

the result may not be ideal. In this paper, probability density estimation is used to calculate the possibility that each pixel belongs to cerebral gray matter (cerebral white matter and cerebrospinal fluid). As a priori knowledge, the probability density estimation of pixel x is calculated based on Gaussian mixture model (GMM), that is:

$$P(x) = \sum_{k=1}^{K} p(k)p(x \mid k), \sum_{k=1}^{K} p(k) = 1, p(k) \in [0,1] \tag{10}$$

Where $p(k)$ is the weight coefficient of the $k\text{-}th$ Gaussian probability estimation model; $p(x|k)$ is the probability estimation model of the $k\text{-}th$ pixel, which is defined as:

$$p(x \mid k_i) = \frac{1}{\sqrt{2\pi\delta^2}} e^{\left(-\frac{(x-u)^2}{2\delta^2}\right)} \tag{11}$$

Among them, δ Represents covariance, μ Indicates data expectations. Using this model, the membership degree of each pixel corresponding to each part of brain tissue can be obtained, and the fitted curve is shown in Fig. 7.
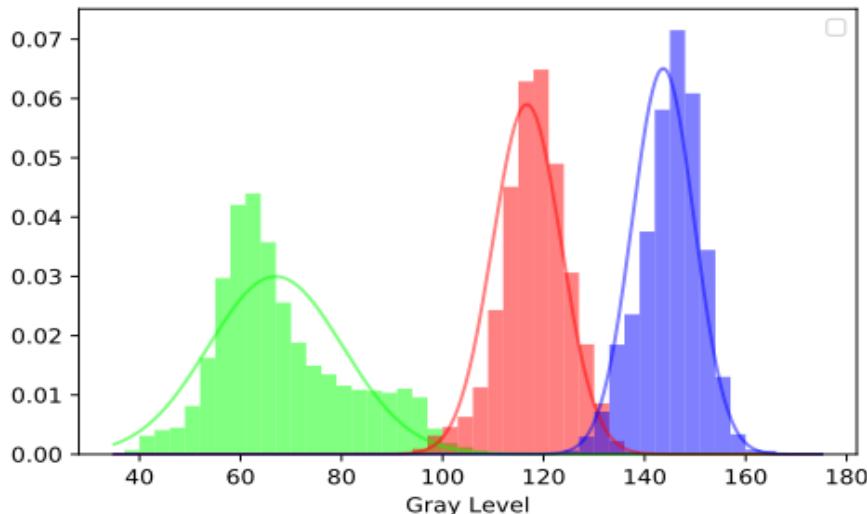

Fig. 7 Gaussian mixture model fitting curve

2.3.3 Super pixel segmentation based on probability density weighted linear spectral clustering

Specifically, p-LSC not only calculates the traditional color values *l, a, b* and Euclidean distances *x* and *y*, but also maps the probability value of each point on the image belonging to brain white matter to the high-dimensional space as an information feature. Here, taking gray matter as an example, for a pixel, after knowing its gray value, the probability that the pixel belongs to gray matter $P_{k_1}(x)$ is

$$P_{k_1}(x) = \frac{p(x|k_1)}{\sum_{i=1}^{3} p(x|k_i)} \tag{12}$$

Among researchers of brain tissue segmentation, Ki refers to three categories: gray matter, white matter and cerebrospinal fluid. Here, it is assumed that K1 is cerebral gray matter, and P (x|k1) represents

the possible probability value when pixel x belongs to cerebral gray matter. However, it should be noted that since the brain MR image is a gray image, only the brightness l in the LAB model is recorded as the gray intensity g.

For the two pixel points m and n in the image, after obtaining four characteristic gray values g_m and g_n, probability densities p_m and p_n, coordinate positions (xm, ym), (xn, yn) respectively, the similarity W of the two points is evaluated by measuring the gray similarity W_g, membership similarity W_p and spatial distance W_d. The formula of p-LSC is redefined as

$$\omega(m) = \sum_{n \in V} \left\{ \alpha \cos \frac{\pi}{2}(g_m - g_n) + \beta \cos \frac{\pi}{2}(p_m - p_n) + \gamma \left(\cos \frac{\pi}{2}(x_m - x_n) + \cos \frac{\pi}{2}(y_m - y_n) \right) \right\}$$

(13)

Among them, α、β、γ The weights of the feature categories are tested step by step to determine the best value. The corresponding mapping function can be further deduced in combination with equation ϕ (6) (7):

$$\phi(m) = \frac{1}{\omega(m)} \begin{pmatrix} \alpha \cos \frac{\pi}{2} g_m, \alpha \sin \frac{\pi}{2} g_m, \beta \cos \frac{\pi}{2} p_m, \beta \sin \frac{\pi}{2} p_m, \\ \gamma \cos \frac{\pi}{2} x_m, \gamma \sin \frac{\pi}{2} x_m, \gamma \cos \frac{\pi}{2} y_m, \gamma \sin \frac{\pi}{2} y_m \end{pmatrix}$$

(14)

The specific flow of p-LSC algorithm is as follows:

In the feature space of the eight dimensional vector corresponding to the mapping of each point $m = (g_m, p_m, x_m, y_m)$ in the image, K seed points $\phi(m)$ are set up at equal intervals horizontally and vertically to move the seed points and find 3×3 the lowest point of the gradient in the neighborhood;

Initialize: initialize the maximum number of iterations, the weighted mean of each cluster seed point and μ_k the search center m_k;

Set label $L\ (m) = 0$ and distance $D\ (m) = \infty$ for each pixel m;

while iter<=MaxIterr

Calculate the v_x of m at $m_k \times$ The distance between $D = \phi(m)$ and μ_k in vy neighborhood;

if $D < d(m)$

$d(m)=D, L(m)=k$

End   if

Update the weighted mean and search center of all clusters;

$iter = iter + 1$

Merge smaller superpixel blocks.

3. Brain MR image segmentation method combining DA-Unet and Superpixel

Although the current full convolution network model based on Unet has good segmentation effect, there are still some problems, such as shallow model depth, insufficient image feature information extraction and large information loss in the process of encoding and decoding, resulting in poor edge contour effect. After

comparing Fig. 5, it can be observed that using the segmentation results of DA-Unet, there is a large error in the edge of a small cerebrospinal fluid in the gray matter compared with the standard segmentation image. Here, the mapping method is used. When p-LSC performs image segmentation, the segmented images of DA-Unet are input at the same time to distinguish the center of gravity of each pixel block. The brain tissue of the pixel block is determined by the category of the pixel points at the same position on the DA-Unet output image. In this way, the high accuracy of DA-Unet segmentation and the characteristics of high Superpixel edge fit and clear contour are used to improve the segmentation accuracy of brain MR image. However, it should be noted that due to the small size of brain MR images in the database, the direct use of Superpixel segmentation is not ideal. Here, the bilinear interpolation method is used to double the preprocessed image and DA-Unet based image, and then Superpixel segmentation and mapping classification are carried out. The specific process is as follows:

(1) Preprocess the original image.

(2) DA-Unet is used to segment brain MR images.

(3) The preprocessed image is doubled by bilinear interpolation. Set the number of seed points n, p-LSC Superpixel segmentation is performed on the expanded image to obtain N pixel blocks, and each pixel block will be marked with the same label $L\ (N)$.

(4) Bilinear interpolation is used to double the gray scale of DA-Unet output. Then, the image is mapped to the Superpixel segmented image, the pixel blocks under the label are classified according to the category of the center of gravity pixel of the pixel block, and the completed image is output.

4. Experimental results and comparative analysis

4.1 Dataset and experimental environment

The brain MR images used in the experiment are from BRAINWEB database [18], which contains 20 simulated T1 weighted simulated brain images, and each image voxel is 256 × two hundred and fifty-six × 181。 In this paper, an image is selected at an interval of 10 pixels from 65 to 120 layers of each data Z axis. There are 7 images for each data, a total of 140 images for brain tissue segmentation. Considering the hardware limitation, 40 of the 84 images of 12 data are selected as the training set, and 30 of the 56 images of the remaining 8 data are selected as the test set.Brain MR image segmentation based on dense Unet is implemented under the tensorflow framework of Win10 system, and the hardware configuration is Inteli7-9700 CPU and NVIDIA RTX 2060S. Image preprocessing and other subsequent operations are carried out on MATLAB R2016b.

4.2 Evaluation index

In order to evaluate the effect of this method more objectively, the following three indicators are used to evaluate the Superpixel segmentation algorithm: under segmentation error (UE) [17], which is used to measure the error after the Ground Truth coincides with the actual output result. boundary recall (BR) [17] is used to measure the ratio of the actually segmented Superpixel block boundary to the Ground Truth boundary. The segmentation accuracy (ASA) [17] is used to measure the percentage of the actual segmentation area in the standard result. The larger the BR, the more accurate the edge segmentation, the lower the UE and the higher the ASA, the less the number of pixels incorrectly segmented and the higher the accuracy.

For the evaluation method of the final segmentation result of brain MR image, the traditional dice similarity coefficient [19] is adopted here, which takes the segmentation accuracy obtained by calculating

the intersection and union ratio between the actual output and the Ground Truth as the index, which is

$$Dice(A, B) = \frac{2|A \cap|}{|A| + |B|}$$

defined as:. Where, A represents the set of pixels in the actual segmentation classification result, and B is the set of pixels in the Ground Truth. $A \cap B$ represents the set of pixels in the actual segmentation result that conform to the Ground Truth data.

4.3 Experimental results and analysis

In order to better evaluate this method, the commonly used simple linear iterative cluster (SLIC) [20] Superpixel segmentation algorithm is selected as a comparison. The segmentation result is shown in Figure 8.
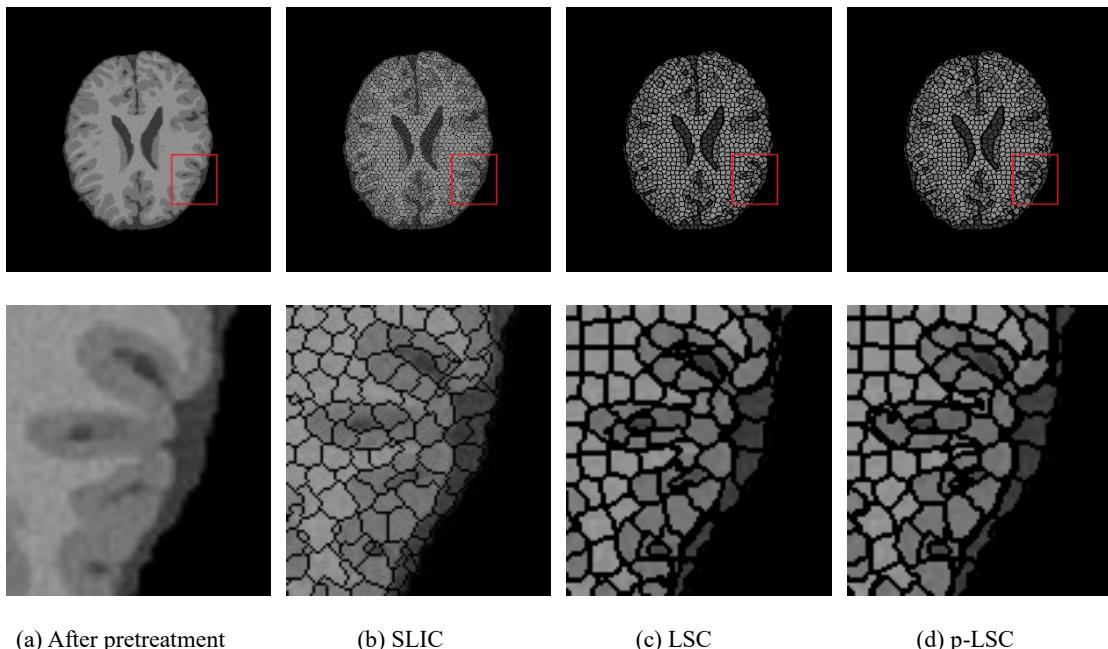

| (a) After pretreatment | (b) SLIC | (c) LSC | (d) p-LSC |

Fig. 8 Comparison of segmentation results of different Superpixel algorithms

Fig. 9 is a broken line diagram drawn according to the indexes of UE, BR and ASA after pixel block segmentation of different orders of magnitude on brain MR images. Combined with the segmentation effect of Fig. 8 and the index results of Fig. 9, it can be seen that the Superpixel segmentation algorithm based on SLIC has a good segmentation effect for different tissues with obvious gray difference, but the effects of parts with similar gray values and edge regions of different tissues, such as the edge zone of gray matter and white matter and small pieces of cerebrospinal fluid in gray matter, are not ideal. Compared with LSC and p-LSC, when the number of segmentation is small, the difference between them is not obvious, but with the increase of the number of segmented Superpixel blocks, the advantage of p-LSC begins to appear. The latter has higher segmentation accuracy, especially when distinguishing gray matter and white matter, it retains more details, the pixel blocks are more regular and the edge effect is better. Obviously, the improved p-LSC Superpixel segmentation algorithm is more suitable for brain MR image segmentation.

Finally, the segmentation effect of brain MR image combined with DA-Unet and p-LSC super pixels is evaluated, and the traditional segmentation method based on FCM is compared. The results are shown in FIG. 10. It can be seen that the brain tissue based on FCM is affected by noise and so on, and the

segmentation effect is poor. In particular, the pixels with fuzzy internal segmentation in the gray matter are seriously Missegmented. Compared with the results of DA-Unet in 2.2.4, the method of DA-Unet + p-LSC has little difference on the whole, but it can be observed in the enlarged picture that the boundary segmentation effect is closer to the standard segmentation result and the integrity is better. The Superpixel segmentation method improves the edge effect of DA-Unet to a certain extent and makes the details more accurate.
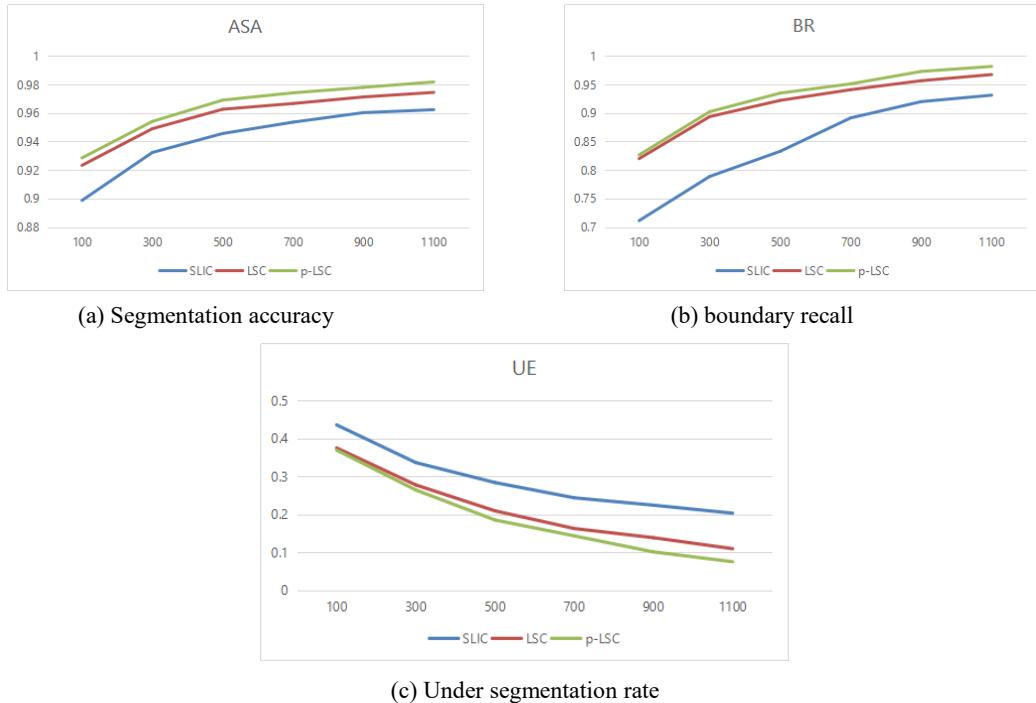

(a) Segmentation accuracy

(b) boundary recall

(c) Under segmentation rate

Fig. 9 Comparison of segmentation performance of different Superpixel algorithms

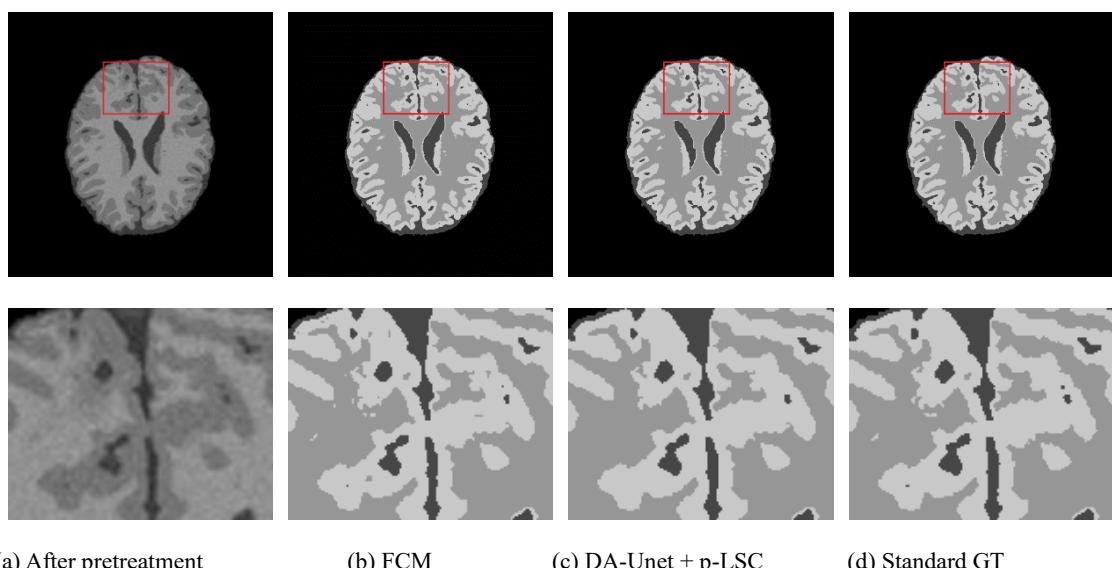(a) After pretreatment (b) FCM (c) DA-Unet + p-LSC (d) Standard GT

Fig. 10 Brain MR image segmentation results under different algorithms

Table 2 Comparison of dice value (%) of brain tissue segmentation results by different methods

Dice	Cerebral white matter	Cerebral gray matter	cerebrospinal fluid
FCM	87.76	87.04	86.31
Unet	89.58	88.13	89.81
NLFCM[21]	95.97	95.11	94.78
DSFCM_N[22]	92.91	94.43	92.70
The proposed DA-Unet	96.06	95.46	94.47
DA-Unet+p-LSC	97.44	97.07	95.95

Table 2 gives the accuracy indexes of brain tissue segmentation results based on different methods, and lists the segmentation results of other papers in recent years as a reference. For those using Jaccard coefficient index, it is unified as Dice coefficient index for comparison. It can be seen that Unet has higher accuracy in brain tissue segmentation of different parts compared with FCM, but there is still much room for improvement. NLFEM and DSFEM_N is two improved fuzzy clustering algorithms for FCM according to different schemes. Compared with the traditional FCM algorithm, the improved NLFEM and DSFEM_N has better anti-interference and stability, and its accuracy has been greatly improved compared with FCM in the segmentation effect of each organization. But on the whole, the two methods proposed in this paper are obviously better. Compared with other methods, the brain tissue accuracy of DA-Unet is improved. The proposed DA-Unet combined with p-LSC was further improved by 1.5% compared with DA-Unet alone. Experiments show that DA-Unet + p-LSC method has high applicability for brain tissue segmentation in brain MR images.

5. Conclusion

In this paper, a brain MR image segmentation method based on improved Unet network and Superpixel is proposed. Firstly, referring to DenseNet, ASPP module and other models, the Unet network is improved, and DA-Unet is proposed to train and segment brain MR images. At the same time, the membership degree of pixels in the image is estimated by probability density based on a priori conditions. The membership degree is used as a new feature information to improve the LSC, and a linear spectral clustering Superpixel segmentation algorithm based on probability density weighting is proposed. Using the high segmentation accuracy of DA-Unet network and the characteristics of strong edge fit and clear contour of p-LSC, the two are combined by mapping. The experimental results show that compared with the traditional methods, the proposed method can better segment the tissue components in brain MR images, and verify the effectiveness of this method.

Acknowledgements

References

[1] Dubey Y K, Mushrif M M. FCM clustering algorithms for segmentation of brain MR images. Advances in Fuzzy Systems, 2016, (3):1-14.

[2] Thirumurugan P, Shanthakumar P. Brain tumor detection and diagnosis using ANFIS classifier. International Journal of Imaging Systems & Technology, 2016, 26(2):157-162.

[3] Sujji G E, Lakshmi Y V S, Jiji G W. MRI brain image segmentation based on thresholding. International Journal of Advanced Computer Research, 2013, 3(1):97-101.

[4] Sandra González-Villà, Oliver A, Valverde S, et al. A review on brain structures segmentation in magnetic resonance imaging. Artificial Intelligence in Medicine, 2016, 73(C):45-69.

[5] Vovk U, Pernus F, Likar B. A review of methods for correction of intensity inhomogeneity in MRI. IEEE Transactions on Medical Imaging, 2007, 26(3):405-421.

[6] Miao Zhengfei, Chen Guanghao, Gao Wei A fully automatic brain MR image segmentation algorithm, China Medical equipment, 2017, 32 (11): 61-65

[7] Zhou Wengang, sun Ting, Zhu Hai An image segmentation algorithm based on adaptive spatial information improved FCM [J] Computer application research, 2015, 32 (007): 2205-2208

[8] Zong Yongsheng, Hu Xiaohui, Qu Yingzhao Kernel FCM Image segmentation algorithm combined with spatial neighborhood information, Computer applications and software, 2017, 34 (04): 221-225 + 333

[9] Wang Yuli, Zhao Zijian Overview of brain image segmentation algorithms based on deep learning, Journal of Biomedical Engineering, 2020, 37 (04): 721-729735

[10] Cao Z H, Qin Y H, Chen Y J. A Multi-Scale Fully Convolutional Networks Model for Brain MRI Segmentation. Journal of Information and Computing Science, 2018, 13(2):083-088.

[11] Xue Huan Research on brain MR image segmentation method based on full convolution neural network, Central China Normal University, 2019

[12] Zhu guanfei, Xu yongqiu, MI Hongmei, et al Extraction method of MR brain tissue based on gray histogram, Computer measurement and control, 2017, 025 (011): 170-173178

[13] Ronneberger O, Fischer P, Brox T, et al. U-Net: Convolutional networks for biomedical image segmentation. Medical Image Computing and Computer Assisted Intervention, 2015:234-241.

[14] Huang G, Liu Z, Van Der Maaten L, et al. Densely connected convolutional networks, Proceedings of the IEEE Conference on Computer Vision and Pattern Recognition, 2017: 4700-4708.

[15] Chen L C, Papandreou G, Kokkinos l, et al. DeepLab: semantic image sementation with deep convolutional nets, atrousconvolution, and fully connected CRFs. IEEE Transactions on Pattern Analysis & Machine Intelligence, 2017, 40(4):834-848.

[16] Berman M, Triki A R, Blaschko M B. The Lovasz-Softmax Loss: A Tractable Surrogate for the Optimization of the Intersection-Over-Union Measure in Neural Networks, 2018 IEEE/CVF Conference on Computer Vision and Pattern Recognition (CVPR). IEEE, 2018.

[17] Chen J S, Li Z Q, Bo H. Linear spectral clustering superpixel. IEEE Transaction on Image Process, 2017, 26(7):3317-3330.

[18] Chris A C, Vasken K, Remi K-S K, et al. Brainweb: online interface to a 3D MRI simulated brain database. NeuroImage, 1997,(5): 425

[19] Zheng Wei, Yao Jizhi, Wang Jie, Liu shuaiqi, Zhang Xiaodan, Ma zepeng Research on MRI brain image segmentation based on fuzzy entropy clustering and improved particle swarm optimization, Laser journal, 2021,42 (01): 98-103

[20] Achanta R, Shaji A, Smith K, et al. SLIC superpixels compared to state-of-the-art superpixel methods. IEEE Transactions on Pattern Analysis and Machine Intelligence, 2012, 34(11):2274-2282.

[21] Zhang X, Sun X, Wang G, et al. Improved fuzzy clustering algorithm withnon-local information for image segmentation. Multimedia Tools and Applications,2016,76（6）：1-27.

[22] Zhang Y, Bai X, Fan R, et al. Deviation-Sparse Fuzzy C-Means With NeighborInformation Constraint. IEEE Transactions on FuzzySystems,2019,27（1）：185-199.